

COLOR IMAGE SET RECOGNITION BASED ON QUATERNIONIC GRASSMANNIANS

XIANG XIANG WANG AND TIN-YAU TAM

ABSTRACT. We propose a new method for recognizing color image sets using quaternionic Grassmannians, which use the power of quaternions to capture color information and represent each color image set as a point on the quaternionic Grassmannian. We provide a direct formula to calculate the shortest distance between two points on the quaternionic Grassmannian, and use this distance to build a new classification framework. Experiments on the ETH-80 benchmark dataset show that our method achieves good recognition results. We also discuss some limitations in stability and suggest ways the method can be improved in the future.

1. INTRODUCTION

Recognizing image sets is an important task in computer vision, with applications in areas such as face recognition, object tracking, and video analysis. In recent years, various methods have been developed using Grassmannians for image set recognition, where image sets are represented as subspaces in higher-dimensional spaces [20, 22]. Although these methods have been successful, many current techniques for handling color images still rely on traditional methods that treat the RGB channels separately. While this can work in certain situations, it misses the connections between the color channels, making it harder to capture the full structure of the color images.

Quaternions, which extend complex numbers into four dimensions, offer a useful approach by allowing all three RGB channels to be stored together in one quaternionic matrix. This provides a compact way to store the data while keeping the relationships between the color channels, making it a more efficient and meaningful representation for color images [14, 17]. By embedding color images into quaternionic Grassmannians, we can take advantage of both quaternions and Grassmannians, creating a powerful method for recognizing image sets.

One of the key challenges in this area is figuring out how to measure distances between points in quaternionic Grassmannian space. These distance measurements are important for comparing image sets and performing classification. Finding a way to reliably and efficiently calculate the distance between two points in quaternionic Grassmannians has been a long-standing problem. To address this, we provide a clear mathematical expression for the shortest geodesic distance between two points in quaternionic Grassmannian space, using matrices. This distance formula is central to our new framework for recognizing color image sets.

Key words and phrases. Quaternionic Grassmannian, Color Image Set, Shortest Geodesic, Image Recognition.

The rest of this paper is organized as follows: Section 2 reviews background information and related work on the quaternion algebra for color image representation and the quaternionic unitary group. In Section 3, we present the mathematical details of how to calculate the shortest distance in quaternionic Grassmannians. Section 4 describes our proposed framework for recognizing color image sets. Section 5 shows experimental results that demonstrate how well our method works. Finally, Section 6 discusses future work.

2. BACKGROUND

In this section, we provide a overview of quaternion algebra for color image representation and quaternionic unitary group. We adhere to the standard notations listed in Table 1 to ensure clarity and consistency.

Symbol	Name
I	The identity matrix with the size $n \times n$
\mathbb{R}	The set of all real numbers
\mathbb{C}	The set of all complex numbers
\mathbb{H}	The set of all quaternion numbers
\mathbb{F}	Represents either \mathbb{R} , \mathbb{C} or \mathbb{H}
$\mathbb{F}_{n \times m}$	The set of all matrices with the size $n \times m$ in \mathbb{F}
\mathbb{F}_n or $\mathbb{F}_{n \times 1}$	The set of all vectors with the size n in \mathbb{F}
M	A smooth manifold
$T_x M$	The tangent space of M at point $x \in M$
$U(n)$	Unitary group
$\mathfrak{s}_{\mathbb{H}}(n)$	The space of $n \times n$ skew quaternionic Hermitian matrices
$U_{\mathbb{H}}(n)$	Quaternionic unitary group
$\mathbf{Gr}_{n,k}(\mathbb{F})$	Grassmannian with k -dimensional subspaces in \mathbb{F}_n
S_n	The space of $n \times n$ real symmetric matrices
H_n	The space of $n \times n$ Hermitian matrices
Q_n	The space of $n \times n$ quaternionic Hermitian matrices
$\ \cdot\ _F$	Frobenius norm
$\ \cdot\ _{\mathbb{H}}$	Frobenius norm for quaternionic matrix
$\mathfrak{u}(n)$	The set of $n \times n$ skew Hermitian matrices
$\exp(\cdot)$ or e^{\cdot}	Exponential map of the matrix
χ_H	The complex representation of the quaternionic matrix H
\cdot^*	The transpose and conjugate notation
$\bar{\cdot}$	The conjugate notation

TABLE 1. Notations used in this paper

2.1. Quaternion Algebra for Color Image Representation. Quaternions, introduced by Hamilton in 1843 [9], extend complex numbers to four dimensions and have found applications in various fields, including computer graphics [19, 13], robotics [2],

and signal processing [26]. In the context of image processing, quaternions offer a unified way to represent color images by encoding the RGB channels into a single quaternion-valued matrix [14, 17]. A quaternion $q \in \mathbb{H}$ is typically written as:

$$q = q_0 + q_1i + q_2j + q_3k,$$

where q_0, q_1, q_2 , and q_3 are real numbers, and i, j , and k are the basis elements satisfying the fundamental relations:

$$i^2 = j^2 = k^2 = ijk = -1.$$

The conjugate of q , denoted as \bar{q} , is defined by

$$\bar{q} = q_0 - q_1i - q_2j - q_3k,$$

and the norm of q is defined as

$$|q| = \sqrt{q\bar{q}} = \sqrt{q_0^2 + q_1^2 + q_2^2 + q_3^2}.$$

For any nonzero quaternion $q \neq 0$, the inverse of q , denoted as q^{-1} , is given by the formula

$$q^{-1} = \frac{\bar{q}}{|q|^2}.$$

Extending the definition of the quaternion number to matrices, a quaternionic matrix $H \in \mathbb{H}_{n \times m}$ is expressed as:

$$H = H_0 + H_1i + H_2j + H_3k,$$

where H_0, H_1, H_2 , and H_3 are real matrices in $\mathbb{R}_{n \times m}$. Alternatively, the matrix H can also be written as:

$$H = (H_0 + H_1i) + (H_2 + H_3i)j,$$

which is a convenient form for deriving its complex representation. The complex representation of the quaternionic matrix H , denoted as χ_H , is defined by:

$$\chi_H = \begin{bmatrix} H_0 + H_1i & H_2 + H_3i \\ -(\overline{H_2 + H_3i}) & \overline{H_0 + H_1i} \end{bmatrix} = \begin{bmatrix} H_0 + H_1i & H_2 + H_3i \\ -H_2 + H_3i & H_0 - H_1i \end{bmatrix}.$$

This complex representation preserves several important properties of quaternionic matrices, as outlined in the following proposition.

Proposition 2.1 (Lee, 1948 [15]). Let $A, B \in \mathbb{H}_{n \times n}$. Then

- $\chi_{AB} = \chi_A \chi_B$;
- $\chi_{A+B} = \chi_A + \chi_B$;
- $\chi_{A^*} = (\chi_A)^*$;
- $\chi_{A^{-1}} = (\chi_A)^{-1}$ if A^{-1} exists;
- χ_A is unitary, Hermitian, or normal if and only if A is unitary, Hermitian, or normal, respectively.

Moving forward, we introduce the concept of “standard eigenvalues” for quaternionic matrices, which are crucial for understanding their spectral properties and have significant applications.

Definition 2.2 (Brenner, 1951; Lee, 1948 [6, 15]). For any $n \times n$ quaternionic matrix A , there exist exactly n (right) eigenvalues that are complex numbers with non-negative imaginary parts. These eigenvalues are referred to as the *standard eigenvalues* of A .

The following lemma offers a good understanding of these eigenvalues and highlights key properties of the eigenvalue structure for related complex matrices.

Lemma 2.3 (Lee, 1949 [15]). Let A and B be $n \times n$ complex matrices. Then, for the block matrix:

$$\begin{pmatrix} A & B \\ -\bar{B} & \bar{A} \end{pmatrix},$$

every real eigenvalue (if any) appears an even number of times, while the complex eigenvalues occur in conjugate pairs.

This observation leads to the following corollary regarding the eigenvalues of quaternionic matrices.

Corollary 2.4. Let $H \in \mathbb{H}^{n \times n}$ be a quaternionic matrix, and let χ_H denote its complex representation. Then χ_H has exactly $2n$ complex eigenvalues, which are symmetrically distributed with respect to the real axis in the complex plane. Among these, exactly n eigenvalues lie in the closed upper half-plane (i.e., the set of complex numbers with non-negative imaginary part). These n eigenvalues are referred to as the *standard eigenvalues* of H , and they correspond to the eigenvalues of χ_H located in the upper half-plane.

Further details can be found in the proof of Theorem 5.4 in [25].

Remark 2.5. Two quaternions q and p are said to be similar if there exists a nonzero quaternion s such that:

$$p = s^{-1}qs.$$

As a result, similar quaternions have the same norm, since the norm is preserved under similarity transformations.

In the context of quaternionic matrices, any right eigenvalue is similar to a standard eigenvalue. This is why standard eigenvalues are often preferred in analysis: once the n standard eigenvalues are obtained, they represent all possible right eigenvalues through similarity transformations.

The spectral properties of quaternionic matrices, especially their standard eigenvalues, are useful in many real-world applications. One important area where quaternion algebra shows its value is in color image processing.

In color image representation, each pixel of a color image can be represented by a pure quaternion, where the components q_1 , q_2 , and q_3 correspond to the values of the red, green, and blue channels, respectively. Consequently, a color image of size $n \times m$ can be represented as a pure $n \times m$ quaternionic matrix (see Figure 1), with each entry in the matrix being a pure quaternion that encodes the RGB information of the corresponding pixel.

This quaternion-based representation enables compact and unified processing of the color channels while preserving the relationships between them. However, most existing approaches using quaternions focus on pixel-wise operations or per-image tasks, rather

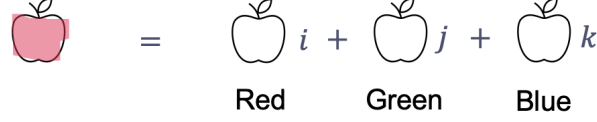


FIGURE 1. A color image represented as a pure quaternionic matrix

than extending the representation to sets of images. This motivates the use of quaternionic Grassmannians, where image sets are treated as subspaces in a quaternionic vector space.

2.2. Quaternionic Unitary Group. We now turn our attention to the quaternionic unitary group $U_{\mathbb{H}}(n)$, which plays a fundamental role in the study of quaternionic Grassmannians. Understanding the geometric structure of $U_{\mathbb{H}}(n)$ is essential because it helps us define and study quaternionic Grassmannians in Section 3. To build this foundation, we first introduce the tangent space and geodesics of $U_{\mathbb{H}}(n)$.

The tangent space of $U_{\mathbb{H}}(n)$ at the identity matrix I is given by:

$$\mathfrak{s}_{\mathbb{H}}(n) = \{H \in \mathbb{H}_{n \times n} : H^* = -H\},$$

which can be derived as follows.

Assume $S \in T_I U_{\mathbb{H}}(n)$, and suppose that there exists a curve $\gamma(t) \in U_{\mathbb{H}}(n)$ such that $\gamma(0) = I$ and $\dot{\gamma}(0) = S$. Since $\gamma(t)$ lies in $U_{\mathbb{H}}(n)$, it satisfies the unitary condition $\gamma(t)^* \gamma(t) = I$. Differentiating this relation with respect to t at $t = 0$ yields [24]:

$$\dot{\gamma}^*(0) + \dot{\gamma}(0) = 0,$$

which implies that $S^* = -S$. Hence, we have $T_I U_{\mathbb{H}}(n) \subset \mathfrak{s}_{\mathbb{H}}(n)$.

Conversely, for any $S \in \mathfrak{s}_{\mathbb{H}}(n)$, consider the curve $\gamma(t) = \exp(tS)$. This curve satisfies $\gamma(0) = I$, $\dot{\gamma}(0) = S$, and the unitary condition $\gamma(t)^* \gamma(t) = I$ holds for all t . Therefore, $\gamma(t)$ lies entirely within $U_{\mathbb{H}}(n)$, which implies that $S \in T_I U_{\mathbb{H}}(n)$. Combining both directions, we conclude that:

$$T_I U_{\mathbb{H}}(n) = \mathfrak{s}_{\mathbb{H}}(n).$$

Moreover, the tangent space of $U_{\mathbb{H}}(n)$ at an arbitrary point $Q \in U_{\mathbb{H}}(n)$ can be expressed as:

$$T_Q U_{\mathbb{H}}(n) = \{QX : X \in \mathfrak{s}_{\mathbb{H}}(n)\}.$$

Having established the structure of the tangent space, we now turn to the characterization of geodesics in $U_{\mathbb{H}}(n)$. For Lie groups equipped with bi-invariant metrics, geodesics correspond to one-parameter subgroups [1, Chapter 2]. Since $U_{\mathbb{H}}(n)$ is a Lie group with a bi-invariant metric, the geodesic starting from $Q \in U_{\mathbb{H}}(n)$ in the direction of $QX \in T_Q U_{\mathbb{H}}(n)$ is given by:

$$\gamma(t) := Q \exp(tX), \quad t \in [0, 1].$$

This geometric framework for $U_{\mathbb{H}}(n)$ will serve as the basis for defining and analyzing quaternionic Grassmannians in the next section.

3. QUATERNIONIC GRASSMANNIAN

Quaternionic Grassmannian $\mathbf{Gr}_{n,k}(\mathbb{H})$ is the set of all k -dimensional subspaces in \mathbb{H}_n and we can define the quaternionic Grassmannian as a set of quaternionic matrices by orthogonal projection matrices in $\mathbb{H}_{n \times n}$:

$$\mathbf{Gr}_{n,k}(\mathbb{H}) = \{P \in \mathbb{H}_{n \times n} : P^2 = P, P^* = P, \text{rank } P = k\},$$

which is equivalent to the quotient space

$$U_{\mathbb{H}}(n)/(U_{\mathbb{H}}(k) \times U_{\mathbb{H}}(n-k)),$$

where $U_{\mathbb{H}}(n) = \{U \in \mathbb{H}_{n \times n} : U^*U = UU^* = I_n\}$ is the quaternionic unitary group.

3.1. Tangent space and geodesic of $\mathbf{Gr}_{n,k}(\mathbb{H})$. We now derive the tangent space and the geodesic form of $\mathbf{Gr}_{n,k}(\mathbb{H})$ based on $U_{\mathbb{H}}(n)$. Consider a curve starting from a point $P \in \mathbf{Gr}_{n,k}(\mathbb{H})$, parameterized as $\alpha(t) = \beta(t)P\beta(t)^*$ with $\alpha(0) = P$, where $\beta(t) \in U_n(\mathbb{H})$ and $\beta(0) = I$.

Since the tangent space of $U_{\mathbb{H}}(n)$ at I is $\mathfrak{s}_{\mathbb{H}}(n)$, we have $\dot{\beta}(0) = X \in \mathfrak{s}_{\mathbb{H}}(n)$ and the tangent vector is $\dot{\alpha}(0) = [X, P]$. Therefore, the tangent space at $P \in \mathbf{Gr}_{n,k}(\mathbb{H})$ is

$$T_P \mathbf{Gr}_{n,k}(\mathbb{H}) = \{[X, P] : X \in \mathfrak{s}_{\mathbb{H}}(n)\}.$$

To emphasize the roles of P and Q in the tangent vector, we write respectively the tangent vector of the geodesic from P to Q and the tangent vector from Q to P as

$$\overrightarrow{PQ} = [X_{PQ}, P], \quad \overrightarrow{QP} = [X_{PQ}, Q].$$

Since each $P \in \mathbf{Gr}_{n,k}(\mathbb{H})$ is a Hermitian quaternionic matrix with eigenvalues consisting of k ones and $n-k$ zeros, the spectral decomposition of $P = U_P P_0 U_P^*$ yields the following map:

$$\pi : U_{\mathbb{H}}(n) \rightarrow \mathbf{Gr}_{n,k}(\mathbb{H}), U \rightarrow U P_0 U^*,$$

which is surjective.

A similar approach to the complex grassmannian case in [4] allows us to express the tangent space of the quaternionic Grassmannian as follows

$$T_P \mathbf{Gr}_{n,k}(\mathbb{H}) = \{[X, P] : X \in \text{Ad}(U_P)\mathfrak{p}_*\},$$

where

$$\mathfrak{p}_* : \left\{ \begin{pmatrix} 0 & Y_1 \\ -Y_1^* & 0 \end{pmatrix} : Y_1 \in \mathbb{H}_{k \times (n-k)} \right\} \subset \mathfrak{s}_{\mathbb{H}}(n),$$

and $\text{Ad}(U)X = UXU^{-1}$.

Furthermore, the geodesic starting from P in the direction $[X, P]$, where $X = U_P \hat{X} U_P$ and $\hat{X} \in \mathfrak{p}_*$ in $\mathbf{Gr}_{n,k}(\mathbb{H})$ can be derived from the corresponding curve in $U_{\mathbb{H}}(n)$ with the form $U_P \hat{X}$. Thus, the geodesic of the grassmannian is

$$\gamma(t) = \exp(tX)P \exp(-tX).$$

3.2. The shortest distance of two points in $\mathbf{Gr}_{n,k}(\mathbb{H})$. For any tangent vector $[X, P] \in T_P \mathbf{Gr}_{\mathbb{H}}$ of $P \in \mathbf{Gr}_{n,k}(\mathbb{H})$, the following properties hold: (1) $X = PX + XP$; (2) $[X, P] = (I - 2P)X = -X(I - 2P)$; (3) $\exp(X)P - P\exp(-X) = \sinh M$. These results can be proved from Lemma 2.1 and Lemma 3.2 in reference [3]. Furthermore, following Theorem 3.3 in [3], for any two points $P, Q \in \mathbf{Gr}_{n,k}(\mathbb{H})$, the geodesic connecting P and Q is given by

$$\gamma(t) = \exp(tX)P\exp(-tX),$$

where the matrix X satisfies

$$\exp(2X) = (I - 2Q)(I - 2P).$$

To further analyze distances on $\mathbf{Gr}_{n,k}(\mathbb{H})$, we rely on the Frobenius norm of quaternionic matrices. This norm is defined based on the singular value decomposition (SVD) of quaternionic matrices, which was established in [25].

Theorem 3.1 (Singular-Value Decomposition [25]). Let $A \in \mathbb{H}_{n \times m}$ be of rank r . Then there exist quaternionic unitary matrices $U \in \mathbb{H}_{n \times n}$ and $V \in \mathbb{H}_{m \times m}$ such that

$$UAV = \begin{pmatrix} D_r & 0 \\ 0 & 0 \end{pmatrix},$$

where $D_r = \text{diag}\{d_1, \dots, d_r\}$ and the d 's are the positive singular values of A .

The singular values obtained from the SVD form the basis for defining the Frobenius norm of quaternionic matrices. Specifically, for a quaternionic matrix $A \in \mathbb{H}_{n \times m}$ of rank r , the Frobenius norm is defined as

$$\|A\|_{\mathbb{H}} = \sqrt{\sum_{i,j} |a_{ij}|^2} = \sqrt{\sum_{k=1}^r \sigma_k^2(A)}, \quad A = (a_{ij}) \in \mathbb{H}_{n \times m},$$

where $\sigma_1(A), \dots, \sigma_r(A)$ are the nonzero singular values of A .

With this norm in place, we can now define the distance between two points $P, Q \in \mathbf{Gr}_{n,k}(\mathbb{H})$. The distance is given by

$$d(P, Q) = \|[X, P]\|_{\mathbb{H}} = \|X\|_{\mathbb{H}},$$

where X is the matrix associated with the geodesic connecting P and Q .

This leads us to the following theorem, which provides an explicit expression for the shortest distance between any two points in $\mathbf{Gr}_{n,k}(\mathbb{H})$.

Let $X \in \mathbf{U}_{\mathbb{H}}(n)$, and let $\hat{\lambda}(X) = (\hat{\lambda}_1(X), \dots, \hat{\lambda}_n(X))$ be the set of standard eigenvalues of X . For any complex number c on the unit circle, we can express $c = e^{i\alpha}$ with $\alpha \in [-\pi, \pi]$. Denote $\overline{\text{arg}}(c) = \alpha$ as the argument of c . In particular, for $c = -1$, we can take either π or $-\pi$ as its argument, that is, $\overline{\text{arg}}(-1) = \pi$ or $-\pi$.

Theorem 3.2. Let P and Q be two points in $\mathbf{Gr}_{n,k}(\mathbb{H})$. Then the shortest distance between P and Q is

$$\hat{d}(P, Q) = \frac{1}{2} \sqrt{\sum_i \overline{\text{arg}}^2(\hat{\lambda}_i((I - 2Q)(I - 2P)))}. \quad (3.1)$$

Proof. Suppose that there are t geodesics between P and Q . The geodesic connecting P and Q with the tangent vector $[X_i, P]$ is given by:

$$\gamma(t) = \exp(tX_i)P \exp(-tX_i), \quad \text{for } i = 1, 2, \dots, t.$$

The distance between P and Q along the geodesic with the tangent vector $[X_i, P]$ at the point P is:

$$d_i(P, Q) = \|[X_i, P]\|_{\mathbb{H}} = \|X_i\|_{\mathbb{H}}.$$

Thus, the shortest distance between P and Q is:

$$\hat{d}(P, Q) = \min_i d_i(P, Q) = \min_i \|X_i\|_{\mathbb{H}}.$$

For each X_i , we have the following relation:

$$\exp(2X_i) = (I - 2Q)(I - 2P).$$

Since $(I - 2Q)(I - 2P)$ is a quaternionic unitary matrix, the eigenvalues $\hat{\lambda}_i((I - 2Q)(I - 2P))$ are complex numbers on the unit circle, and the remaining right eigenvalues are similar to the standard eigenvalues. Let us write the eigenvalues as:

$$\hat{\lambda}_i((I - 2Q)(I - 2P)) = \exp(ia_i),$$

where $a_i \in [-\pi, \pi]$. Since similar eigenvalues have the same norm, we obtain:

$$\min_i \|2X_i\|_{\mathbb{H}} = \sqrt{\sum_i a_i^2}.$$

Therefore, we have

$$\hat{d}(P, Q) = \frac{1}{2} \min_i \|2X_i\|_{\mathbb{H}} = \frac{1}{2} \sqrt{\sum_i \overline{\arg}^2(\hat{\lambda}_i((I - 2Q)(I - 2P)))}.$$

□

Remark 3.3. The distance formula (3.1), which is also compatible with real and complex Grassmannians, is a well-defined metric as it satisfies the three fundamental conditions of a metric space: “non-negativity”, “symmetry”, and the “triangle inequality”. A detailed proof is provided below.

3.3. Proof of the Triangle Inequality for the Distance Formula (3.1). It is straightforward to verify that the non-negativity and symmetry conditions hold for the distance formula. To complete the proof that it is a well-defined metric, we need to establish the triangle inequality. To do this, we first introduce some key properties of the complex Grassmannian $\mathbf{Gr}_{n,k}(\mathbb{C})$, which will help guide our approach. We consider the model of Grassmannians as the set of orthogonal projection matrices in $\mathbb{C}_{n \times n}$ of rank k :

$$\mathbf{Gr}_{n,k}(\mathbb{C}) = \{P \in \mathbb{C}_{n \times n} : P^2 = P, P^* = P, \text{rank } P = k\},$$

which is the subset of the space of $n \times n$ Hermitian matrices.

The properties of $\mathbf{Gr}_{n,k}(\mathbb{C})$ have been well studied, particularly in [5] and [3], and we will use some of their results in our proof.

First, the tangent space of any point $P \in \mathbf{Gr}_{n,k}(\mathbb{C})$ is given by

$$T_P \mathbf{Gr}_{n,k}(\mathbb{C}) = \{[X, P] = (I - 2P)X = -X(I - 2P) : X \in \mathfrak{u}(n)\},$$

where $\mathfrak{u}(n)$ is the space of skew-Hermitian matrices. Next, from Proposition 3.2 in [5] and [3] we know that for a point $P \in \mathbf{Gr}_{n,k}(\mathbb{C})$ with a tangent vector $\overrightarrow{PQ} = [X, P]$, the geodesic $\gamma(t)$ is given by

$$\gamma(t) = \exp(tX)P \exp(-tX),$$

where $Q = \exp(X)P \exp(-X)$ and \exp denotes the matrix exponential function. Moreover, for every $P \in \mathbf{Gr}_{n,k}(\mathbb{C})$, there is a $U_P \in \mathrm{U}(n)$ such that $P = U_P P_0 U_P^{-1}$ by the Spectral Decomposition of Hermitian matrices, where

$$P_0 := \begin{pmatrix} I_k & 0 \\ 0 & 0 \end{pmatrix} \in \mathbf{Gr}_{n,k}(\mathbb{C}).$$

With this spectral decomposition, we can further refine the description of the tangent space.

Proposition 3.4. For every $P \in \mathbf{Gr}_{n,k}(\mathbb{C})$, let $U_P \in \mathrm{U}(n)$ such that $P = U_P P_0 U_P^{-1}$. Then

$$\begin{aligned} T_P \mathbf{Gr}_{n,k}(\mathbb{C}) &= \left\{ \left[U_P \begin{pmatrix} 0 & Y_1 \\ -Y_1^* & 0 \end{pmatrix} U_P^{-1}, P \right] : Y_1 \in \mathbb{C}_{k \times (n-k)} \right\} \\ &= [\mathrm{Ad}(U_P) \mathfrak{p}_*, P], \end{aligned}$$

where

$$\mathfrak{p}_* := \left\{ \begin{pmatrix} 0 & Y_1 \\ -Y_1^* & 0 \end{pmatrix} : Y_1^* \in \mathbb{C}_{(n-k) \times k} \right\} \subset \mathfrak{u}(n).$$

Proof. Suppose $P = U_P P_0 U_P^{-1}$. Given $X \in \mathfrak{u}(n)$, express it as

$$X = U_P \begin{pmatrix} X_1 & Y_1 \\ -Y_1^* & Z_1 \end{pmatrix} U_P^{-1}, \quad X_1 \in \mathfrak{u}(n), \quad Z_1 \in \mathfrak{u}(n-k), \quad Y_1 \in \mathbb{C}_{k \times (n-k)}$$

so

$$[X, P] = U_P \begin{pmatrix} 0 & -Y_1 \\ -Y_1^* & 0 \end{pmatrix} U_P^{-1} = \left[U_P \begin{pmatrix} 0 & Y_1 \\ -Y_1^* & 0 \end{pmatrix} U_P^{-1}, P \right] \quad (3.2)$$

and

$$XP + PX = U_P \begin{pmatrix} 2X_1 & Y_1 \\ -Y_1^* & 0 \end{pmatrix} U_P^{-1}. \quad (3.3)$$

Then

$$T_P \mathbf{Gr}_{n,k}(\mathbb{C}) = \left\{ \left[U_P \begin{pmatrix} 0 & Y_1 \\ -Y_1^* & 0 \end{pmatrix} U_P^{-1}, P \right] : Y_1 \in \mathbb{C}_{k \times (n-k)} \right\}.$$

So we can restrict the choices of $X \in \mathfrak{u}(n)$ to a smaller set $\mathrm{Ad}(U_P) \mathfrak{p}_* \subset \mathfrak{u}(n)$, where

$$\mathfrak{p}_* := \left\{ \begin{pmatrix} 0 & Y_1 \\ -Y_1^* & 0 \end{pmatrix} : Y_1^* \in \mathbb{C}_{(n-k) \times k} \right\} \subset \mathfrak{u}(n).$$

Thus

$$T_P \mathbf{Gr}_{n,k}(\mathbb{C}) = \{[X, P] : X \in \mathrm{Ad}(U_P) \mathfrak{p}_*\}.$$

□

Proposition 3.5. Let $P, Q \in \mathbf{Gr}_{n,k}(\mathbb{C})$. Let $\gamma(t)$ be the geodesic joining $\gamma(0) = P$ and $\gamma(1) = Q$. Then there exists a $\tilde{X}_{PQ} \in \mathfrak{p}_*$ such that $[\text{Ad}(U_P^{-1})\tilde{X}_{PQ}, P]$ is the tangent vector to γ at P , and there is $U_Q \in \text{U}(n)$ such that $U_Q P_0 U_Q^{-1} = Q$ and

$$e^{\tilde{X}_{PQ}} = U_P^{-1} U_Q. \quad (3.4)$$

Proof. As $\text{ad } P : \text{Ad}(U_P)\mathfrak{p}_* \rightarrow T_P \mathbf{Gr}_{n,k}(\mathbb{C})$ is surjective, there is a $\tilde{X}_{PQ} \in \mathfrak{p}_*$ such that $\overrightarrow{PQ} = [\text{Ad}(U_P^{-1})\tilde{X}_{PQ}, P]$ is the tangent vector to the geodesic $\gamma(t)$ at P . The map

$$\pi : \text{U}(n) \rightarrow \mathbf{Gr}_{n,k}(\mathbb{C}), \quad U \rightarrow U P_0 U^{-1}$$

is surjective and $\mathbf{Gr}_{n,k}(\mathbb{C}) = \pi(\text{U}(n))$ is the orbit of P_0 under the adjoint action of $\text{U}(n)$. Then from the directional derivative of π at U_P , we can find a geodesic $\hat{\gamma}(t) := U_P e^{t\tilde{X}_{PQ}}$ in $\text{U}(n)$ with the tangent vector $U_P \tilde{X}_{PQ}$ at U_P such that

$$\pi(\hat{\gamma}(t)) = \gamma(t)$$

and $U_Q := \hat{\gamma}(1)$. When $t = 1$, we have

$$e^{\tilde{X}_{PQ}} = U_P^{-1} U_Q.$$

□

To prove the triangle inequality, we use the following result from Thompson.

Theorem 3.6 (Thompson, 1986). Let $A, B \in \mathbb{C}_{n \times n}$ be skew-Hermitian matrices. Then there exist unitary matrices $X, Y \in \text{U}(n)$ (depending on A and B) such that:

$$e^A e^B = e^{XAX^{-1} + YBY^{-1}}. \quad (3.5)$$

We would like to highlight that the relation in (3.5) also holds for quaternionic matrices in \mathbb{H} , and this can be proved using the properties of the complex matrix representation of quaternions, as discussed in [18]. With all these tools in place, we can now state and prove the main result in the complex Grassmannians first.

Theorem 3.7. Let $P, Q, R \in \mathbf{Gr}_{n,k}(\mathbb{C})$. Then

$$\hat{d}(P, Q) \leq \hat{d}(Q, R) + \hat{d}(R, P).$$

Proof. By Proposition 3.5, we can find U_P, \hat{U}_P, U_Q and U_R such that

$$e^{\tilde{X}_{PQ}} = U_P^{-1} U_Q, \quad e^{\tilde{X}_{QR}} = U_Q^{-1} U_R, \quad e^{\tilde{X}_{RP}} = U_R^{-1} \hat{U}_P,$$

where $U_P P_0 U_P^{-1} = \hat{U}_P P_0 \hat{U}_P^{-1} = P$, $U_Q P_0 U_Q^{-1} = Q$, and $U_R P_0 U_R^{-1} = R$. Assume that $\hat{U}_P = U_P W$ and

$$W := \begin{bmatrix} W_k & \\ & W_{n-k} \end{bmatrix} \quad W_k \in \text{U}(k), W_{n-k} \in \text{U}(n-k).$$

Then

$$e^{\tilde{X}_{PQ}} e^{\tilde{X}_{QR}} e^{\tilde{X}_{RP}} = W, \quad (3.6)$$

where $\tilde{X}_{PQ}, \tilde{X}_{QR}, \tilde{X}_{PR} \in \mathfrak{p}_*$. Moreover, for any $X \in \mathbb{C}_{n \times n}$, $e^X = \sinh X + \cosh X$, $\sinh X = \frac{e^X - e^{-X}}{2}$ and $\cosh X = \frac{e^X + e^{-X}}{2}$. From (3.6), we have

$$\begin{aligned} & \sinh(\tilde{X}_{PQ}) \sinh(\tilde{X}_{QR}) \sinh(\tilde{X}_{RP}) + \sinh(\tilde{X}_{PQ}) \cosh(\tilde{X}_{QR}) \cosh(\tilde{X}_{RP}) \\ & + \cosh(\tilde{X}_{PQ}) \sinh(\tilde{X}_{QR}) \cosh(\tilde{X}_{RP}) + \cosh(\tilde{X}_{PQ}) \cosh(\tilde{X}_{QR}) \sinh(\tilde{X}_{RP}) = 0, \end{aligned}$$

and

$$e^{\tilde{X}_{PQ}} e^{\tilde{X}_{QR}} e^{\tilde{X}_{RP}} = e^{-\tilde{X}_{PQ}} e^{-\tilde{X}_{QR}} e^{-\tilde{X}_{RP}}. \quad (3.7)$$

By (3.7), we have

$$e^{-2\tilde{X}_{PQ}} = e^{\tilde{X}_{QR}} e^{\tilde{X}_{RP}} e^{\tilde{X}_{RP}} e^{\tilde{X}_{QR}}.$$

Apply Theorem 3.6 to get two unitary matrices M_1 and M_2 such that

$$e^{-2\tilde{X}_{PQ}} = e^{2M},$$

where $M = M_1 \tilde{X}_{QR} M_1^* + M_2 \tilde{X}_{RP} M_2^*$. When we only consider the case that all eigenvalues of \tilde{X}_{PQ} , \tilde{X}_{QR} , and \tilde{X}_{RP} are all in $[-\pi, \pi]$, the corresponding distance will be the shortest distances. The relation between eigenvalues of \tilde{X}_{PQ} and M is as following (make sure the eigenvalue of $2\tilde{X}_{PQ}$ is in $[-2\pi, 2\pi]$)

$$\lambda_i(\tilde{X}_{PQ}) = \begin{cases} \lambda_i(M) + 2\pi & \text{if } \lambda_i(M) < -\pi \\ \lambda_i(M) & \text{if } -\pi < \lambda_i(M) < \pi \\ \lambda_i(M) - 2\pi & \text{if } \pi < \lambda_i(M) \end{cases}.$$

Obviously, $\sigma(\tilde{X}_{PQ}) \prec_w \sigma(M)$. So

$$\|\tilde{X}_{PQ}\|_F \leq \|M\|_F = \|M_1 \tilde{X}_{QR} M_1^* + M_2 \tilde{X}_{RP} M_2^*\|_F \leq \|\tilde{X}_{QR}\|_F + \|\tilde{X}_{RP}\|_F,$$

that is,

$$\hat{d}(P, Q) \leq \hat{d}(Q, R) + \hat{d}(R, P).$$

□

Finally, by Proposition 2.1, we can extend this result naturally to quaternionic Grassmannians:

Corollary 3.8. Let $P, Q, R \in \mathbf{Gr}_{n,k}(\mathbb{H})$. Then

$$\hat{d}(P, Q) \leq \hat{d}(Q, R) + \hat{d}(R, P).$$

This completes the proof that the distance formula (3.1) is a valid metric on $\mathbf{Gr}_{n,k}(\mathbb{H})$, satisfying all necessary conditions.

Remark 3.9. The results established in our previous work [21] can be extended to the quaternionic Grassmannian within certain locally convex ball. This extension follows from the properties of the complex representation of quaternionic matrices.

4. COLOR IMAGE SET RECOGNITION BASED ON QUATERNIONIC GRASSMANNIAN

4.1. Grassmannian Representation of a Color Image Set. Each $n \times m$ color digital image is represented as an $n \times m$ quaternionic matrix, where each element in the matrix is a pure quaternion of the form $ri + gj + bk$, where r, g, b are the red, green, and blue channel values of the corresponding pixel.

Consider

$$Z = \begin{bmatrix} r_{11}i + g_{11}j + b_{11}k & \cdots & r_{1m}i + g_{1m}j + b_{1m}k \\ \vdots & \ddots & \vdots \\ r_{n1}i + g_{n1}j + b_{n1}k & \cdots & r_{nm}i + g_{nm}j + b_{nm}k \end{bmatrix} \in \mathbb{H}^{n \times m}.$$

The quaternionic matrix Z encodes the color image compactly by storing the RGB channels together. The image matrix is partitioned into columns z_i and stacked into a long column vector of length nm :

$$[z_1 | z_2 | \cdots | z_m] \rightarrow \mathbf{z} = \begin{bmatrix} z_1 \\ z_2 \\ \vdots \\ z_m \end{bmatrix} \in \mathbb{H}_{nm \times 1}.$$

This column vector \mathbf{z} provides a compact representation of the color image as a single quaternionic vector.

Then, consider a set $\mathcal{A} = \{A_1, A_2, \dots, A_p\}$ of p color images with the same size $t \times m$. Each image can be represented by a quaternionic vector:

$$\mathbf{a}_i \in \mathbb{H}_{tm \times 1}, \quad i = 1, 2, \dots, p.$$

The image set can thus be written as a set of p quaternionic vectors:

$$\{\mathbf{a}_1, \mathbf{a}_2, \dots, \mathbf{a}_p\}.$$

To reduce the dimensionality, we apply Principal Component Analysis (PCA) based on the quaternionic singular value decomposition (QSVD) [14] and retain the top k components, resulting in the reduced set of vectors:

$$\{\hat{\mathbf{a}}_1, \hat{\mathbf{a}}_2, \dots, \hat{\mathbf{a}}_k\}.$$

These vectors span a subspace in the quaternionic vector space. To process the image set, we orthonormalize these vectors using the modified Gram-Schmidt process of Theorem 4.3 in [8] to obtain an orthonormal set:

$$\{\mathbf{a}_1, \mathbf{a}_2, \dots, \mathbf{a}_k\}.$$

The resulting orthonormal vectors form the columns of a matrix $X \in \mathbb{H}_{tm \times k}$:

$$X = [\mathbf{a}_1 | \mathbf{a}_2 | \dots | \mathbf{a}_k].$$

Finally, the quaternionic Grassmannian element representing the color image set is given by:

$$A = XX^* \in \mathbf{Gr}_{tm,k}(\mathbb{H})$$

where A is a projection matrix in the quaternionic Grassmannian $\mathbf{Gr}_{tm,k}(\mathbb{H})$, and it compactly encodes the color image set \mathcal{A} .

Algorithm 1 outlines the procedure for representing a set of color images using quaternionic Grassmannians. Each image is transformed into a quaternionic column vector, and an orthonormal set is derived for efficient representation. The framework is illustrated in the figure 2.

Algorithm 1 Quaternionic Grassmannian Representation of a Color Image Set

- 1: **Input:** A color image set $\mathcal{A} = \{A_1, A_2, \dots, A_p\}$ of p color images with the same size $t \times m$
- 2: Convert each color image into a quaternionic column vector:
- 3: **for** each image A_i **do**
- 4: Partition A_i into columns and stack them into a quaternionic vector $\mathbf{a}_i \in \mathbb{H}_{tm}$.
- 5: **end for**
- 6: Reduce $\{\mathbf{a}_1, \mathbf{a}_2, \dots, \mathbf{a}_p\}$ as $\{\hat{\mathbf{a}}_1, \hat{\mathbf{a}}_2, \dots, \hat{\mathbf{a}}_k\}$ by QSVD.
- 7: Orthonormalize the quaternionic vectors $\{\hat{\mathbf{a}}_1, \hat{\mathbf{a}}_2, \dots, \hat{\mathbf{a}}_k\}$ using the modified Gram-Schmidt process [8] for quaternions to obtain an orthonormal set $\{\mathbf{a}_1, \mathbf{a}_2, \dots, \mathbf{a}_k\}$.
- 8: Form the matrix X with the orthonormal vectors as columns:

$$X = [\mathbf{a}_1 | \mathbf{a}_2 | \dots | \mathbf{a}_k]$$

- 9: Compute the Grassmannian representation A of the image set:

$$A = XX^*$$

- 10: **Output:** The Grassmannian element A , representing the color image set \mathcal{A} .
-

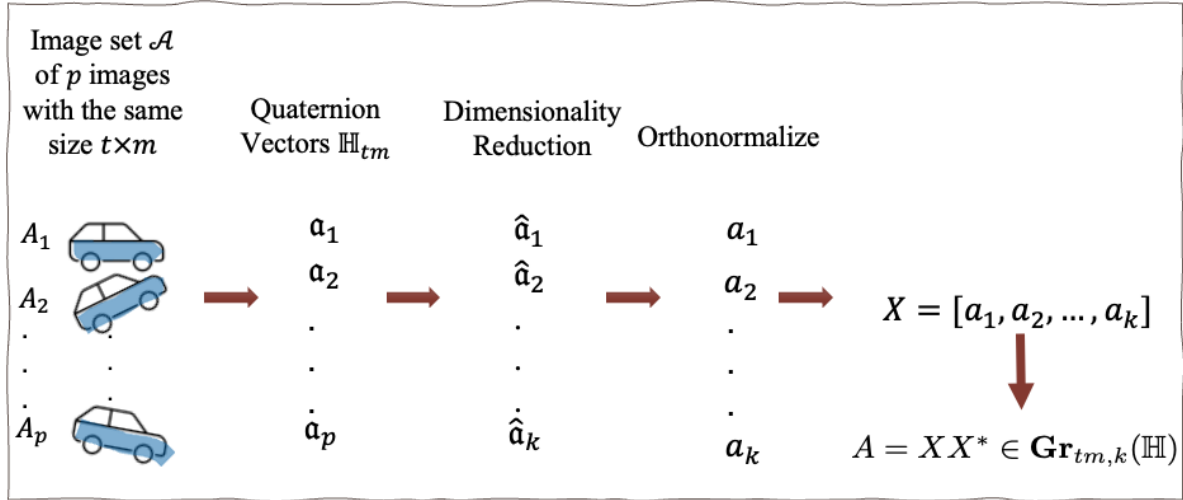


FIGURE 2. Quaternionic Grassmannian representation of a color image set.

4.2. A New Framework for Color Image Set Recognition Based on Quaternionic Grassmannians. Based on the Grassmannian representation of image sets and the distance formula, we propose a new framework for color image set recognition using

quaternionic Grassmannians. As a straightforward example, we consider three image sets belonging to two distinct classes. The recognition process for these three image sets is described in Algorithm 2, and the framework is visually illustrated in Figure 3.

Algorithm 2 Framework for Color Image Set Recognition Using Quaternionic Grassmannians (Three Image Sets)

- 1: **Input:** Three color image sets $\mathcal{A}, \mathcal{B}, \mathcal{C}$, each containing p color images of the same size $n \times m$.
 - 2: Represent the three color image sets in $\mathbf{Gr}_{n,k}(\mathbb{H})$ (the Grassmannian space of quaternionic matrices) using Algorithm 1, obtaining representations A, B, C .
 - 3: Compute the distances $\hat{d}(A, B)$, $\hat{d}(A, C)$, and $\hat{d}(B, C)$.
 - 4: **Output:** The shortest distance identifies one class, and the remaining set belongs to the second class.
-

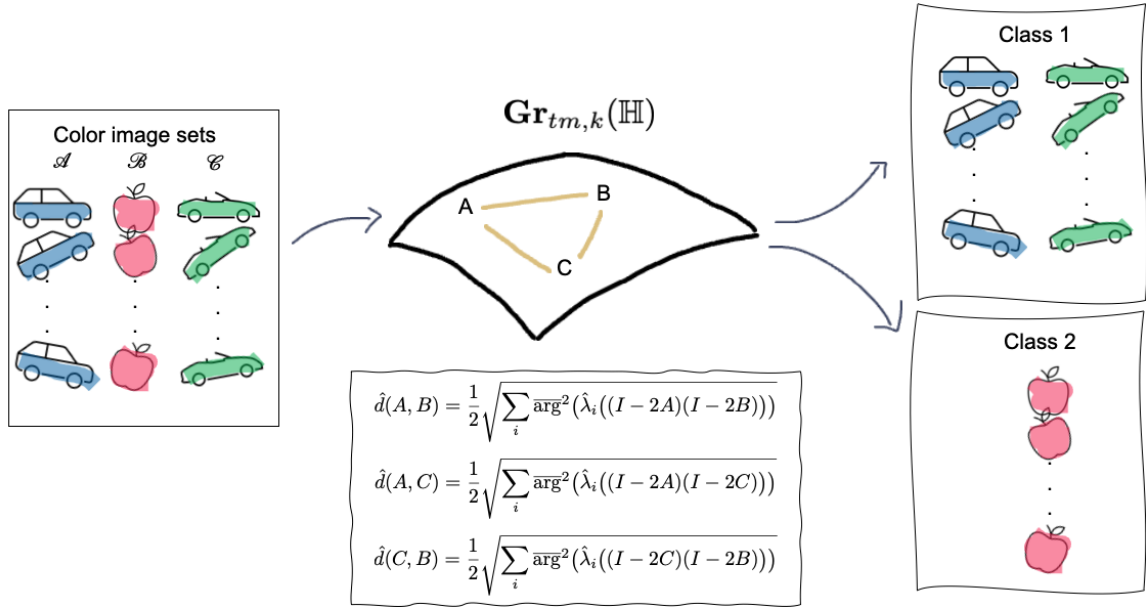


FIGURE 3. Framework for color image set recognition using quaternionic Grassmannians (three image sets)

This framework establishes a fundamental structure for performing color image set recognition based on quaternionic Grassmannians. It provides a theoretical basis for developing more advanced algorithms and methods in future work, enabling more robust and efficient recognition techniques.

5. NUMERICAL EXAMPLE

In this section, we test our new framework using the ETH-80 [dataset](#) [16]. The ETH-80 dataset contains images from eight categories, including apples, pears, and cars. Each

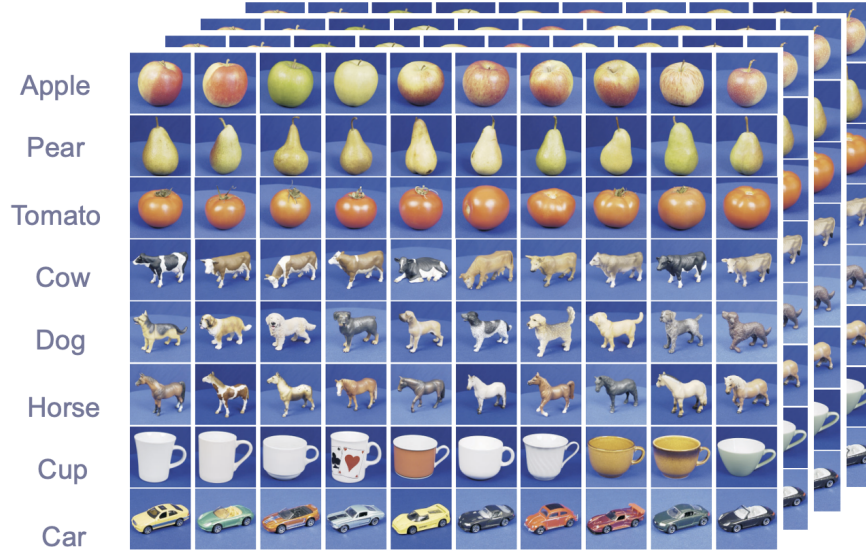


FIGURE 4. The eight categories of the ETH-80 dataset. Each category contains 10 objects with 41 views per object.

category has 10 objects with 41 views per object, resulting in a total of 3280 images. The following figure illustrates the ETH-80 dataset.

For this evaluation, the dataset was divided into training and testing sets. Five sub-categories were used for training, and the remaining five were used for testing, ensuring a balanced and fair evaluation. Each image was resized to 20×20 , with $t = 20$, $m = 20$, and we set $k = 9$. Consequently, the quaternionic Grassmannian considered in this work is $\mathbf{Gr}_{400,9}(\mathbb{H})$.

In Figure 5, the eight categories are represented by clusters, where the training data points form the clusters, and the red point represents a testing sample. To classify the test sample, we computed its distances to each training cluster using the average distances within the quaternionic Grassmannian space. The test sample was then assigned to the category corresponding to the closest cluster.

Using this framework, we computed the distances between points in the quaternionic Grassmannian to classify the test data. The process was repeated 10 times to ensure reliability, and the average recognition rates and standard deviations were calculated. Table 2 presents the average recognition rates and standard deviations (%) for various methods compared with our proposed approach.

Our method achieved an average recognition rate of 97.00% with a standard deviation of $\pm 1.97\%$. While this demonstrates the framework's ability to achieve high accuracy, the relatively large standard deviation indicates some variability in performance.

Despite this variability, we believe our framework shows great potential. Since advanced techniques such as deep learning or feature selection methods have not yet been incorporated, there is significant room for optimization and improvement. Future enhancements could further improve the framework's performance and robustness.

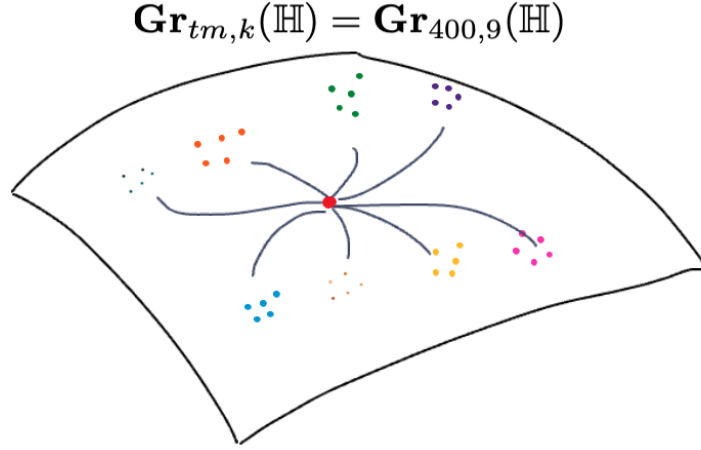


FIGURE 5. Visualization of the eight categories represented by training data points and a single testing data point.

Method	Recognition Rate (%)
GDA [10]	91.00 ± 2.13
GEDA [12]	92.50 ± 1.16
GDL [11]	93.50 ± 0.92
GiFME [7]	74.50 ± 1.22
GGPLCR [23]	96.75 ± 1.30
Our Method	97.00 ± 1.97

TABLE 2. Average recognition rates and standard deviations (%) for various methods compared with our proposed framework.

Remark 5.1. During our experiments, we observed some variations in recognition rates and standard deviations across multiple runs. Specifically, we obtained results such as $93.0 \pm 3.5\%$, $94.5 \pm 3.07\%$, $95.25 \pm 2.75 \%$, $96.75 \pm 2.06 \%$ and $97.25 \pm 2.75 \%$. These fluctuations indicate that while our method achieves high recognition accuracy, its stability could be improved. This suggests that enhancing the robustness of our approach is an important direction for future work.

6. CONCLUSION

This work introduced significant contributions to the recognition of color image sets using quaternionic Grassmannians. We developed an explicit formula for computing the shortest path between points in quaternionic Grassmannians, offering a mathematically sound and efficient approach for distance calculations. Additionally, we proposed a novel framework for color image set recognition that effectively utilizes the structure of quaternionic Grassmannians to handle high-dimensional, multi-channel image data.

Despite these advancements, there is room for further improvement.

- One limitation of our current method is that it relies on computing the standard eigenvalues of quaternionic unitary matrices of the form $(I - 2Q)(I - 2P)$. This step is time-consuming and slows down the process for large image sets. If we can develop faster ways to compute these eigenvalues, our method would work better for large-scale and real-time applications.
- Another direction involves incorporating advanced techniques, such as deep learning and feature extraction, to enhance the robustness and accuracy of the framework. These additions could expand its applicability to more complex and diverse datasets.

By addressing these challenges, this framework has the potential to evolve into a powerful tool for a wide range of applications in computer vision and image processing, contributing to advancements in the field.

APPENDIX A. MATLAB CODES

LISTING 1. Processing Color Image Sets Data

```
% Base directory containing subfolders (1, 2, ..., 8)
base_directory = '/Users/xiangxiang/Library/CloudStorage/OneDrive-
UniversityofNevada,Reno/2024/Fall-2024/Math-799/Quaternion
Grassmannian-in-Image-set-reconignition/Dataset/ETH-80-master
/ETH-80-master';

% List of main directories to process (1 for apples, 2-8 for other
categories)
main_dirs = {'1', '2', '3', '4', '5', '6', '7', '8'};

% Output folder for combined quaternion vectors
output_folder = fullfile(base_directory, 'Combined_Quaternion_Vectors');
if ~exist(output_folder, 'dir')
    mkdir(output_folder);
end

% Process all main directories
for main_dir_idx = 1:length(main_dirs)
    current_dir = fullfile(base_directory, main_dirs{main_dir_idx});
    subdirs = dir(fullfile(current_dir, '*'));
    % Subfolders within the current directory

    % Filter valid subdirectories (exclude '.' and '..')
    subdirs = subdirs([subdirs.isdir] & ~startsWith({subdirs.name}, '.'));

    % Process each subdirectory (e.g., Apple_1, Car_1, etc.)
    for sub_idx = 1:length(subdirs)
        subdir_path = fullfile(current_dir, subdirs(sub_idx).name);
        image_extensions = {'*.jpg', '*.png', '*.bmp', '*.tif'};
```

```

image_files = [];

% Collect image files
for ext = image_extensions
    image_files = [image_files; dir(fullfile(subdir_path, ext{1}))];
end

if isempty(image_files)
    fprintf('No images found in: %s\n', subdir_path);
    continue;
end

% Initialize combined quaternion vector
combined_quaternion_vector = quaternion([], [], [], []);

% Process each image file
for k = 1:length(image_files)
    image_path =
        fullfile(image_files(k).folder, image_files(k).name);
    img = imread(image_path);
    img_resized = imresize(img, [20, 20]);

    % Convert to quaternion matrix
    quaternion_matrix = quaternion(...
        zeros(size(img_resized, 1), size(img_resized, 2)), ...
        double(img_resized(:, :, 1)), ...
        double(img_resized(:, :, 2)), ...
        double(img_resized(:, :, 3)));

    % Flatten into vector and append
    quaternion_vector = quaternion_matrix(:);
    combined_quaternion_vector =
        [combined_quaternion_vector quaternion_vector];
end

% Save combined quaternion vector
category_info =
    sprintf('%s-%s', main_dirs{main_dir_idx}, subdirs(sub_idx).name);
output_file = fullfile(output_folder, [category_info, '.mat']);
save(output_file, 'combined_quaternion_vector', 'category_info');
fprintf('Processed and saved quaternion vector for %s\n', category_info);
end
end

disp('All categories processed, quaternion vectors saved.');
```

% Orthogonalize and compute projector matrices

```

mat_files = dir(fullfile(output_folder, '*.mat'));

```

```

orthogonal_output_directory = fullfile(output_folder ,
'Orthogonalized-Matrices');
projector_output_directory = fullfile(output_folder ,
'Projector-Matrices');

if ~exist(orthogonal_output_directory , 'dir'), mkdir(orthogonal_output_directory);
end
if ~exist(projector_output_directory , 'dir'), mkdir(projector_output_directory);
end
t=9;
for k = 1:length(mat_files)
    % Load combined quaternion vector
    mat_file_path = fullfile(mat_files(k).folder , mat_files(k).name);
    data = load(mat_file_path);
    quaternion_matrix0 = data.combined_quaternion_vector;

    % Input: quaternion_matrix0 (n x m), k = target # of components

quaternion_matrix= QuaternionPCA_Column(quaternion_matrix0 , t);

[n, m] = size(quaternion_matrix);

% Initialize orthogonalized matrix
orthogonal_matrix = quaternion(zeros(n, m), zeros(n, m), zeros(n, m), zeros(n, m));
q_1 = QuaternionReal(quaternion_matrix(:, 1));
q_1 = q_1 / normQ(q_1);
orthogonal_matrix(:, 1) = RealQuaternion(q_1);

% Gram-Schmidt Process
for i = 2:m
    q_i = QuaternionReal(quaternion_matrix(:, i));
    for j = 1:i-1
        q_j = QuaternionReal(orthogonal_matrix(:, j));
        projection = timesQ(q_j, timesQ(transQ(q_j), q_i));
        q_i = q_i - projection; % Remove projection
    end
    q_i_norm = normQ(q_i);
    if q_i_norm > 0
        q_i = q_i * (1 / q_i_norm);
    else
        error('Zero-norm-encountered.-Check-input-vectors-for-linear-dependence. ');
    end
    orthogonal_matrix(:, i) = RealQuaternion(q_i);
end

% Compute projector matrix

```

```

projector_matrix = timesQ(QuaternionReal(orthogonal_matrix),
    transQ(QuaternionReal(orthogonal_matrix)));

% Save orthogonalized and projector matrices
[~, name, ~] = fileparts(mat_files(k).name);
save(fullfile(orthogonal_output_directory, [name, '_Orthogonalized.mat']),
    'orthogonal_matrix');
save(fullfile(projector_output_directory, [name, '_Projector.mat']),
    'projector_matrix');
fprintf('Processed and saved matrices for: %s\n', name);
end

disp('Orthogonalization and projector matrices saved. ');

% Compute distances between projector matrices
projector_files = dir(fullfile(projector_output_directory, '*_Projector.mat'));
num_files = length(projector_files);
distance_matrix = zeros(num_files);

% Load projector matrices into memory
projector_matrices = cell(num_files, 1);
file_names = cell(num_files, 1);
for k = 1:num_files
    data = load(fullfile(projector_files(k).folder, projector_files(k).name));
    projector_matrices{k} = data.projector_matrix;
    file_names{k} = projector_files(k).name;
end

% Compute distances
[nq, ~] = size(projector_matrices{1});
I = [eye(nq) zeros(nq) zeros(nq) zeros(nq)];
for i = 1:num_files
    for j = i+1:num_files
        P_i = projector_matrices{i};
        P_j = projector_matrices{j};
        diff_matrix = timesQ((I - 2 * P_i), (I - 2 * P_j));
        eigenvalues = quaternion_eigenvalues(RealQuaternion(diff_matrix));
        d = pick_unique_values_with_duplicates(eigenvalues);
        distance_matrix(i, j) = norm(log(d));
        distance_matrix(j, i) = distance_matrix(i, j);
    end
end

disp('Distance Matrix: ');
disp(distance_matrix);

% Display pairwise distances

```

```

for i = 1:num_files
    for j = i+1:num_files
        fprintf( 'Distance between %s and %s: %.6f\n', file_names{i},
                file_names{j}, distance_matrix(i, j));
    end
end

```

LISTING 2. Classification Algorithm

```

% Parameters
num_categories = 8; % Updated for 10 categories
num_elements_per_category = 10;
k = 5; % Number of training elements per category
m = 10; % Number of trials
target_accuracy = 50.0; % Target accuracy threshold
max_attempts = 1000; % Maximum number of repetitions to find a valid set

% Distance matrix
a = load( 'distance_matrixPCA.mat' );
distance_matrix = a.distance_matrix;

% Store results that meet the accuracy threshold
successful_accuracy_results = [];

for attempt = 1:max_attempts
    % Store accuracy for each trial
    accuracy_results = zeros(m, 1);

    for trial = 1:m
        % Initialize training and testing indices
        training_indices = cell(num_categories, 1);
        testing_indices = cell(num_categories, 1);

        % Randomly split the data into training and testing sets for each category
        for category = 1:num_categories
            % Get the indices for the current category
            category_indices = (category - 1) * num_elements_per_category
                               + (1:num_elements_per_category);

            % Shuffle the indices
            shuffled_indices = category_indices(randperm(num_elements_per_category));

            % Split into training and testing sets
            training_indices{category} = shuffled_indices(1:k);
            testing_indices{category} = shuffled_indices(k+1:end);
        end

        % Perform classification for each test element

```

```

num_test_elements = (10 - k) * num_categories;
predicted_labels = zeros(num_test_elements, 1);
true_labels = repelem(1:num_categories, 10 - k)';
test_counter = 0;

for category = 1:num_categories
    for test_idx = testing_indices{category}
        test_counter = test_counter + 1;

        % Average distances to each category's training data
        avg_distances = zeros(num_categories, 1);
        for train_category = 1:num_categories
            train_indices = training_indices{train_category};
            avg_distances(train_category) =
                mean(distance_matrix(test_idx, train_indices));
        end

        % Assign the test element to the category
        %with the minimum average distance
        [~, predicted_labels(test_counter)] = min(avg_distances);
    end
end

    % Compute accuracy for this trial
    accuracy_results(trial) = mean(predicted_labels == true_labels) * 100;
end

    % Calculate average accuracy for this attempt
    average_accuracy = mean(accuracy_results);
    std_accuracy = std(accuracy_results);

    % Check if the average accuracy meets the target threshold
    if average_accuracy >= target_accuracy
        successful_accuracy_results = accuracy_results;
        fprintf('Found a successful attempt with
        -----Average Accuracy: %.2f%%\n', average_accuracy);
        break;
    end
end

if isempty(successful_accuracy_results)
    fprintf('No successful attempt found after %d repetitions.\n', max_attempts);
else
    % Display successful results
    fprintf('Successful Average Accuracy
    ----- over %d trials: %.2f%%\n', m, average_accuracy);
    fprintf('Standard Deviation of Accuracy:
    ----- +- %.2f%%\n', std_accuracy);

```

```

% Plot accuracy distribution
histogram(successful_accuracy_results , 'Normalization', 'probability');
xlabel('Accuracy-(%)');
ylabel('Frequency');
title('Accuracy-Distribution-for-Successful-Attempt');
grid on;
end

```

LISTING 3. PCA on Quaternionic Column Vectors

```

function Z = QuaternionPCA_Column(Q, t)
% QuaternionPCA_Column – Perform PCA on quaternion column vectors
% Q : m N quaternion matrix (each column is a quaternion vector of length m)
% t : reduced dimension (t < m)
% Z : t N reduced quaternion vectors
% U : m t quaternion projection matrix
[m, N] = size(Q);
% Step 1: Mean Centering
Q_mean = mean(Q, 2); % m 1
Q_c = Q - Q_mean * ones(1, N); % m N centered quaternion matrix

% Step 2: Quaternion covariance matrix: C = Q_c * Q_c^H
Q_cR=QuaternionReal(Q_c);
Q_cHR=transQ(Q_cR); % Hermitian transpose (conjugate + transpose)
C = timesQ(Q_cHR, Q_cR);
% m m quaternion covariance matrix
CQ=RealQuaternion(C);
% Step 3: Convert quaternion covariance to complex 2m 2m matrix
[U,D,V]= svd(CQ); % complex surrogate matrix

% sort by eigenvalue

V_t = U(:, 1:t); % select top t components

V_tR=QuaternionReal(V_t);
% Step 6: Project centered quaternion vectors to reduced space
ZR = timesQ(Q_cR, V_tR);
Z=RealQuaternion(ZR); % t N reduced quaternion matrix
end

```

REFERENCES

- [1] M. M. Alexandrino and R. G. Bettiol. *Lie Groups with Bi-invariant Metrics*, pages 27–47. Springer International Publishing, Cham, 2015.
- [2] S. L. Altmann. *Rotations, Quaternions, and Double Groups*. Clarendon Press, 1986.

- [3] E. Batzies, K. Hüper, L. Machado, and F. Silva Leite. Geometric mean and geodesic regression on Grassmannians. *Linear Algebra Appl.*, 466:83–101, 2015.
- [4] T. Bendokat, R. Zimmermann, and P.-A. Absil. A grassmann manifold handbook: Basic geometry and computational aspects. *arXiv preprint arXiv:2011.13699*, 2020.
- [5] T. Bendokat, R. Zimmermann, and P.-A. Absil. A grassmann manifold handbook: basic geometry and computational aspects. *Advances in Computational Mathematics*, 50(6), 2024.
- [6] J. L. Brenner. Matrices of quaternions. *Pacific Journal of Mathematics*, 1:329–335, 1951.
- [7] R. Chakraborty and B. C. Vemuri. Recursive fréchet mean computation on the grassmannian and its applications to computer vision. In *Proceedings of the 2015 IEEE International Conference on Computer Vision (ICCV)*, ICCV ’15, page 4229–4237, USA, 2015. IEEE Computer Society.
- [8] D. R. Farenick and B. A. Pidkowich. The spectral theorem in quaternions. *Linear Algebra and its Applications*, 371:75–102, 2003.
- [9] W. R. Hamilton. On quaternions; or on a new system of imaginaries in algebra. *The London, Edinburgh, and Dublin Philosophical Magazine and Journal of Science*, 25(163):10–13, 1844.
- [10] J. Hamm and D. D. Lee. Grassmann discriminant analysis: a unifying view on subspace-based learning. In *Proceedings of the 25th international conference on Machine learning*, pages 376–383, 2008.
- [11] M. Harandi, C. Sanderson, C. Shen, and B. Lovell. Dictionary learning and sparse coding on grassmann manifolds: An extrinsic solution. In *Proceedings of the 2013 IEEE International Conference on Computer Vision, ICCV ’13*, page 3120–3127, USA, 2013. IEEE Computer Society.
- [12] M. T. Harandi, C. Sanderson, S. A. Shirazi, and B. C. Lovell. Graph embedding discriminant analysis on grassmannian manifolds for improved image set matching. *CVPR 2011*, pages 2705–2712, 2011.
- [13] J. B. Kuipers. *Quaternions and Rotation Sequences: A Primer with Applications to Orbits, Aerospace, and Virtual Reality*. Princeton University Press, 1999.
- [14] N. Le Bihan and S. J. Sangwine. Quaternion principal component analysis of color images. In *Proceedings 2003 International Conference on Image Processing (Cat. No. 03CH37429)*, volume 1, pages I–809. IEEE, 2003.
- [15] H.-C. Lee. Eigenvalues and canonical forms of matrices with quaternion coefficients. In *Proceedings of the Royal Irish Academy. Section A: Mathematical and Physical Sciences*, volume 52, pages 253–260. JSTOR, 1948.
- [16] B. Leibe and B. Schiele. Analyzing appearance and contour based methods for object categorization. In *2003 IEEE Computer Society Conference on Computer Vision and Pattern Recognition, 2003. Proceedings.*, volume 2, pages II–409, 2003.
- [17] S.-C. Pei and C.-M. Cheng. Color image processing by using binary quaternion-moment-preserving thresholding technique. *IEEE Transactions on image Processing*, 8(5):614–628, 1999.
- [18] L. Rodman. *Topics in quaternion linear algebra*. Princeton Series in Applied Mathematics. Princeton University Press, Princeton, NJ, 2014.
- [19] K. Shoemake. Animating rotation with quaternion curves. *ACM SIGGRAPH Computer Graphics*, 19(3):245–254, 1985.
- [20] L. S. Souza, N. Sogi, B. B. Gatto, T. Kobayashi, and K. Fukui. Grassmannian learning mutual subspace method for image set recognition. *Neurocomputing*, 517:20–33, 2023.
- [21] T.-Y. Tam and X. X. Wang. Geometric properties and distance inequalities on grassmannians, 2024.
- [22] X. Wang, Z. Li, and D. Tao. Subspaces indexing model on grassmann manifold for image search. *IEEE Transactions on Image Processing*, 20(9):2627–2635, 2011.
- [23] D. Wei, X. Shen, Q. Sun, X. Gao, and W. Yan. Prototype learning and collaborative representation using grassmann manifolds for image set classification. *Pattern Recognition*, 100:107123, 2020.
- [24] D. Xu and D. P. Mandic. The theory of quaternion matrix derivatives. *IEEE Transactions on Signal Processing*, 63(6):1543–1556, 2015.
- [25] F. Zhang. Quaternions and matrices of quaternions. *Linear algebra and its applications*, 251:21–57, 1997.

- [26] F. Zhang. Quaternion-based quaternion fourier transform for signal and image processing. *Applied Mathematics and Computation*, 93(2-3):195–205, 1998.

DEPARTMENT OF MATHEMATICS AND STATISTICS, UNIVERSITY OF NEVADA, RENO, RENO, NV
89557-0084, USA

Email address: `xiangxiangw@unr.edu`

DEPARTMENT OF MATHEMATICS AND STATISTICS, UNIVERSITY OF NEVADA, RENO, RENO, NV
89557-0084, USA

Email address: `ttam@unr.edu`